

Wenkun XIE, Fengzhou FANG

# Crystallographic orientation effect on cutting-based single atomic layer removal

© Higher Education Press 2020

**Abstract** The ever-increasing requirements for the scalable manufacturing of atomic-scale devices emphasize the significance of developing atomic-scale manufacturing technology. The mechanism of a single atomic layer removal in cutting is the key basic theoretical foundation for atomic-scale mechanical cutting. Material anisotropy is among the key decisive factors that could not be neglected in cutting at such a scale. In the present study, the crystallographic orientation effect on the cutting-based single atomic layer removal of monocrystalline copper is investigated by molecular dynamics simulation. When undeformed chip thickness is in the atomic scale, two kinds of single atomic layer removal mechanisms exist in cutting-based single atomic layer removal, namely, dislocation motion and extrusion, due to the differing atomic structures on different crystallographic planes. On close-packed crystallographic plane, the material removal is dominated by the shear stress-driven dislocation motion, whereas on non-close packed crystallographic planes, extrusion-dominated material removal dominates. To obtain an atomic, defect-free processed surface, the cutting needs to be conducted on the close-packed crystallographic planes of monocrystalline copper.

**Keywords** ACSM, single atomic layer removal mechanism, crystallographic orientation effect, mechanical cutting, Manufacturing III

Received May 10, 2020; accepted July 1, 2020

Wenkun XIE, Fengzhou FANG (✉)  
Centre of Micro/Nano Manufacturing Technology (MNMT-Dublin),  
University College Dublin, Dublin 4, Ireland  
E-mail: fengzhou.fang@ucd.ie

Fengzhou FANG  
State Key Laboratory of Precision Measuring Technology and  
Instruments, Centre of Micro/Nano Manufacturing Technology  
(MNMT), Tianjin University, Tianjin 300072, China

## 1 Introduction

### 1.1 Scope of atomic and close-to-atomic scale cutting

Atomic and close-to-atomic scale manufacturing (ACSM), i.e., Manufacturing III [1], aims to realize the manufacture of processed surfaces with atomic-scale form accuracy or feature size via material removal, transformation, and addition at atomic and close-to-atomic scales [2]. It will involve the fundamental study, technological development, and engineering applications of the controlled removal, addition, and migration of targeted atoms in Manufacturing III [2], where the external energy directly impacts individual atoms. The behavior of individual atoms is studied, and the relevant manufacturing technologies are developed in ACSM, whereas the collective and continuum material deformation behavior is emphasized in current manufacturing (Manufacturing II).

Mechanical cutting is among the versatile and highly-efficient mechanical machining processes in the industry through which parts with high surface finish or specific functional features are produced. Mechanical cutting has gradually evolved into conventional cutting, microcutting [3–7], and nanocutting [8–10], thereby enabling material removal at the macroscale, microscale, and nanoscale, respectively. However, the microscale in micromachining generally refers to an undeformed chip thickness between 1 and 999  $\mu\text{m}$  [11], whereas the nanoscale in nanocutting typically refers to mechanical cutting with an undeformed chip thickness in the range of 1–100 nm [12].

When the undeformed chip thickness is further decreased to smaller than 1 nm, the materials to be machined would only include several atomic layers and even a single atomic layer, as the lattice distances between two atoms are in the range of 0.2–0.4 nm [13]. At such a small scale, the undeformed chip thickness is comparable to or smaller than workpiece atomic size, thereby leading to the atomic sizing effect on cutting-based material removal with a precision of a single atomic layer [14]. Consequently, a new-generation of cutting, i.e., atomic-

and close-to-atomic-scale (ACS) cutting, needs to be proposed. ACS cutting is kinematically similar to nanometric cutting but fundamentally different from nanometric cutting in many aspects. The scope and context of ACS cutting need to be defined, as they may represent different meanings for different people.

ACS cutting refers to the mechanical machining process, i.e., direct material removal with a precision of single atomic layer, using a geometrically defined cutting edge. It is normally applied to the machining of the parts at atomic and close-to-atomic scales in a variety of engineering materials. It aims to do the following:

1) Produce parts with atomic form accuracy or feature size. The parts could be microscopic or macroscopic.

2) Achieve controlled atomic layer removal by mechanical machining.

The characteristic features that determine and define the scope of ACS cutting are as follows:

- **Undeformed chip thickness.** Currently, no accurate border exists between nanometric and ACS cutting. Fang et al. [12] defined nanometric cutting as mechanical cutting with an undeformed chip thickness in the range of 1–100 nm. By contrast, an undeformed chip thickness of smaller than 1 nm is used in ACS cutting. Thus, the undeformed chip thickness used in ACS cutting would differ from that used in current nanometric cutting, microcutting, and conventional macrocutting, leading to dislocation motion-dominated chip formation [15].

- **Dimension and accuracy of parts.** ACS cutting is used to fabricate the parts with atomic-scale form accuracy or feature size. The atomic-scale feature could be fabricated on normal-sized parts, or micro/nano structured surfaces. For the dimension of part/feature, the parts or features fabricated in ACS cutting must have a dimension accuracy of single atomic layer or several atomic layers and must be smaller than 1 nm; at least one dimension should fall in this range.

- **Cutting tool geometry.** The size and geometry of ACS cutting tools determine the limit of size and accuracy of the feature in ACS. Cutting edge radius, an important geometric parameter of a cutting tool, is usually smaller than 10–20 nm in ACS cutting, thereby allowing controlled atomic layer removal. When a larger cutting edge radius is adopted, only extrusion-dominated material removal could be achieved by mechanical cutting.

Enabling controlled material removal with the ultimate precision of a single atomic layer is extremely challenging.

- **Underlying cutting mechanics.** ACS cutting is not a simple downscaling of microcutting/nanocutting. In ACS cutting, when the undeformed chip thickness becomes comparable with the workpiece atomic diameter or lattice distance between workpiece atoms, a few critical issues, such as workpiece atomic sizing [14], cutting edge radius [16,17], and strain rate effects, would dominate. These sizing effects in ACS cutting would significantly affect the cutting mechanics, including surface generation, chip formation, cutting forces, and subsurface deformation, thereby making ACS cutting significantly different from microcutting/nanocutting and conventional macrocutting.

ACS cutting could be regarded as the fourth generation cutting. It is significant to establish the basic ACS cutting theory and enabling technology to achieve material removal at close-to-atomic scale and even at atomic scale. The combination of research outcomes on ACS cutting mechanism and those on conventional cutting, microcutting, and nanocutting would establish a comprehensive knowledge framework for the research, development, and innovation of mechanical cutting. The basic cutting theory would be established and enriched by different scales, from conventional macroscale, microscale, and nanoscale to the ultimate atomic and close-to-atomic scale.

## 1.2 ACS cutting and nanometric cutting

Researchers would usually compare ACS cutting with nanometric cutting. It is confusing to clearly distinguish ACS cutting from nanometric cutting, and such confusion should be due to the following reasons.

First, no general agreement on the definition of nanometric cutting exists. When the undeformed chip thickness is decreased to nanometric order (1–100 nm), the cutting process could be generally regarded as nanometric cutting, as shown in Table 1. However, even at an undeformed chip thickness of 1 nm, at least several atomic layers are included in the materials to be cut. Based on nanocutting, accurately controlling the movement of each atomic layer is impossible. By contrast, in ACS cutting, only several atomic layers and even a single atomic layer

**Table 1** Comparison of mechanical cutting at different scales

Cutting	Machining objects	Nominal depth of cut	Feature size	Surface finish	Cutting edge radius
ACS cutting	Single atomic layer and at most several atomic layers	$\leq 1$ nm	$< 1$ nm	Atomic	$R < 10\text{--}20$ nm
Nanocutting	At least several atomic layers	1–100 nm [11]	1–100 nm	Nanometric	$R \geq 10\text{--}20$ nm
Microcutting		1–10 $\mu\text{m}$	1–999 $\mu\text{m}$	$< 100$ nm $R_a$	
Ultra-precision cutting		0.10–10 $\mu\text{m}$	1 mm and above	Typically $< 20$ nm $R_a$	

Note:  $R_a$ , surface roughness.

are included in the undeformed chip thickness of smaller than 1 nm. The material removal precision of single atomic layer is the target to be achieved in ACS cutting.

To obtain the processed surface or feature with the ultimate accuracy of a single atomic layer, the workpiece atomic sizing effect on the cutting process should be considered in detail [14].

ACS cutting processes share common characteristics with nanometric cutting, such as cutting edge radius effect and surface generation. However, in ACS cutting, the atomic sizing effect must be considered, as the cutting depth is comparable with or smaller than the workpiece atomic size. The chip formation in ACS cutting needs to be dominated by dislocation motion, in contrast to the extrusion-dominated chip formation in nanocutting.

In nanocutting, the collective behavior of at least several atomic layers is usually the focus of research. In ACS cutting, the individual behavior of a single atomic layer needs to be investigated to achieve the controlled cutting-based atomic layer removal.

### 1.3 State-of-the-art ACS cutting

Mechanical cutting is one of the promising machining processes that enable ACSM via material removal at the atomic scale [18]. To develop ACS cutting technology for the achievement of ACSM, a systematic fundamental understanding of the underlying mechanism of material removal in cutting at the atomic scale is needed. Generally, material deformation and removal in ACS cutting only involve several atomic layers and even a single atomic layer. Currently, directly observing the material removal behavior at the atomic scale is difficult. Molecular dynamics (MD) modelling is a powerful and alternative method for gaining a fundamental understanding of cutting mechanism at micro/nanoscale and even atomic scale [19–21]. Many MD-based analyses are carried out to study the nanocutting mechanism and to accelerate the application of nanocutting-based enabling technology to the academia and industry [22,23]. Recently, MD modelling was used to study the material deformation and removal mechanism at the atomic scale. Chen et al. [24] used MD simulation to analyze the fundamental material removal mechanism in mechanochemical machining to achieve nanomanufacturing with a single atomic layer removal precision. Zhu and Fang [25] also investigated the surface generation and subsurface deformation mechanism in the tip-based mechanical machining process to achieve a single atomic layer removal process. Their outcomes contribute to the establishment and enrichment of the theoretical framework for ACS cutting. Based on MD analysis, we found that as cutting depth decreases to the close-to-atomic scale and even atomic scale, the minimum chip thickness decreases to a single atomic layer when the undeformed chip thickness is approximately 0.2 nm [14]. Moreover, the

underlying ACS cutting mechanic has been systematically investigated from the aspect of chip formation, surface generation, subsurface deformation, and cutting forces. The findings have provided many insights into the mechanism of material deformation and removal at the atomic scale. Significantly different characteristics have been discovered, and current cutting theory is distinguished.

Material anisotropy is one of the material properties that greatly influence the mechanism of cutting at the conventional scale, microscale [26–28], and nanoscale [29–31]. It clearly indicates that the material anisotropy has significantly affected the cutting mechanics from various aspects, such as chip formation [32], surface generation [33], and cutting forces. As only several atomic layers and even one single atomic layer are involved in ACS cutting, the material deformation and removal behavior greatly depend on the atomic arrangement structure of workpiece material.

For the abovementioned reasons, the crystallographic orientation effect on material deformation and removal in ACS cutting is investigated by MD analysis in this study. The research results clearly indicate that due to the crystallographic orientation effect, there are two kinds of mechanisms of material removal in ACS cutting, namely, dislocation motion and extrusion.

---

## 2 Numerical methods

This study aims to analyze the crystallographic orientation effect on material removal mechanism in ACS cutting. The presented MD simulations are implemented by using open-resource computer code LAMMPS [34]. The 3D MD cutting model consists of a diamond cutting tool and a monocrystalline copper workpiece, as depicted in Fig. 1. The model parameters are summarized as follows:

- Configuration: 3D-cutting;
- Tool edge radius: 2 nm;
- Tool material: Diamond;
- Tool dimensions: Rake angle =  $0^\circ$ , relief angle =  $12^\circ$ ;
- Undeformed chip thickness: 0.2 nm;
- Workpiece material: Monocrystalline copper;
- Workpiece dimension:  $37 \text{ nm} \times 9.8 \text{ nm} \times 8 \text{ nm}$ ;
- Potential function used: EAM (copper), Morse (tool-workpiece);
- Cutting speed: 25 m/s;
- Bulk temperature: 293 K.

All MD cutting simulations are conducted on several typical crystallographic planes of monocrystalline copper, including (111), (110), and (001), and the cutting direction is along the orientation of (001)  $\langle \bar{1}00 \rangle$ , (110)  $\langle 00\bar{1} \rangle$ , and (111)  $\langle \bar{1}\bar{1}2 \rangle$ , respectively. The diamond cutting tool is created from a diamond material with an ideal crystalline structure. The rake and clearance angles of the cutting tool

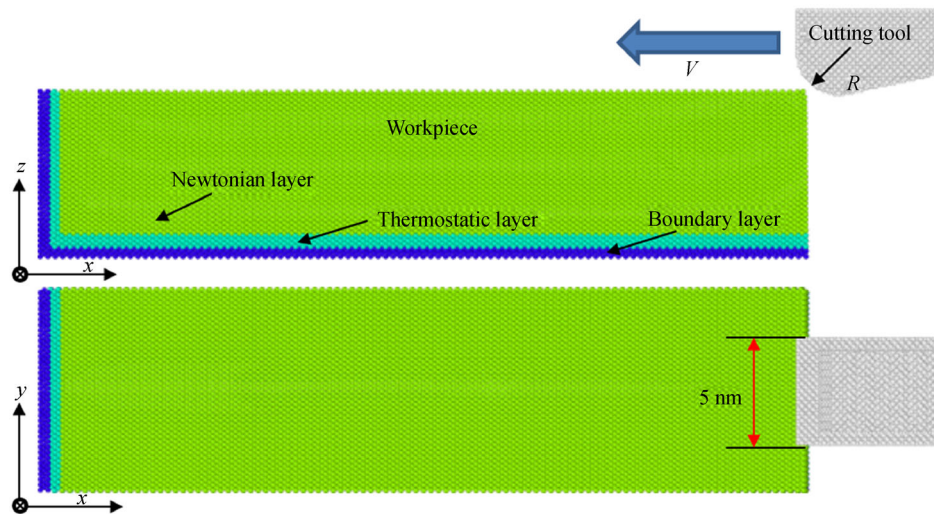


Fig. 1 Molecular dynamics cutting model.

are  $0^\circ$  and  $12^\circ$ . The cutting edge radius used in the present study is 2 nm. In the cutting process, the cutting velocity of 25 m/s is adopted to decrease the computation time. An undeformed chip thickness of 0.2 nm is applied to each case. The dimensions of the workpiece in the  $x$ -,  $y$ -, and  $z$ -direction are  $37 \text{ nm} \times 9.8 \text{ nm} \times 8 \text{ nm}$ . Moreover, the possible effect of the tool nose radius is ignored.

In the MD simulations, the workpiece atoms are divided into three types, namely, Newtonian, thermostatic, and boundary layers. The temperature of the thermostatic layer atoms is maintained at approximately 293 K to simulate the possible heat dissipation in the cutting process. The cutting simulations are conducted after an early-stage relaxation of about 200 ps. The boundary layer atoms are treated as rigid and kept immobilized over the cutting process to eliminate the possible cutting-induced movement of the workpiece surface. As the focus of analysis, the Newtonian layer atoms obey Newtonian laws. All MD simulations are conducted in the NVE ensemble, which includes atom number ( $N$ ), volume ( $V$ ), and energy ( $E$ ). To minimize the boundary effect, the periodical boundary condition is adopted in the  $x$ - and  $y$ -direction, whereas the fixed boundary condition is applied in the  $z$ -direction.

The embedded atom method (EAM) is used to describe the interatomic interaction between copper atoms; EAM has been widely used to describe the surface properties of metal materials [35]. The Morse potential function is applied to calculate the interatomic interaction between copper and diamond atoms [36]. For the interaction among diamond atoms of the cutting tool, the cutting tool is treated as rigid, as diamond materials are much harder than copper atoms. Possible tool wear is not considered in this study.

### 3 Results and discussions

#### 3.1 Chip formation

As shown in Figs. 2(a) and 2(b), chip formation is present on the Cu(111) and Cu(001) surfaces, in front of the rounded cutting edge. By contrast, on the Cu(110) surface, elastic-plastic deformation instead of chip formation is observed within the contact region between the cutting tool and the workpiece. With the advance of the cutting tool, materials are continually pressed to generate a new processed surface. Therefore, due to the crystallographic orientation effect, different cases of chip formations exist even at the same cutting edge radius and undeformed chip thickness. However, the chip formation on Cu(111) surface is conducted via shear stress-driven dislocation motion [14], whereas the extrusion-dominated material removal mechanism dominates the chip formation on the Cu(001) surface, as further analyzed in Section 3.2.

With the advance of the cutting tool, most of the removed workpiece materials on the Cu(111) surface accumulate on the unmachined workpiece surface to generate chips. A small volume of materials flows to both sides of cutting trajectory, as shown in Fig. 3(a). Meanwhile, the defect-free processed surface is successfully obtained.

On the Cu(001) surface, only a small volume of chip is formed ahead of the rounded cutting edge, whereas most of the removed materials form a pile via side-flow, due to the ploughing action of the cutting tool. On the Cu(110) surface, some of the workpiece materials are directly pressed into the processed surface, and the others flow to both sides of the cutting traces.

### 3.2 Surface generation

Different surface morphologies exist on various crystallographic planes even at the same cutting edge radius and process parameters due to the different chip formation mechanisms induced by the crystallographic orientation effect. As shown in Fig. 3(a), on the newly formed processed Cu(111) surface, the defect-free processed surface could be obtained with the ideal crystalline structure. On the Cu(001) and Cu(110) surfaces, many surface defects form on the processed surfaces, including surface atomic vacancies, isolated individual atoms, or atom clusters, as shown in Figs. 3(b) and 3(c). These findings are ascribed to the crystallographic orientation effect on surface generation in cutting-based single atomic layer removal.

Considering that only several atomic layers and even one single atomic layer are involved in the material

removal and surface generation process, this section emphatically investigates the displacement behavior of each atomic layer when the undeformed chip thickness is decreased to the atomic scale. The results are shown in Fig. 4.

In the cutting-based single atomic layer removal process on Cu(111) surface, only the first atomic layer undergoes an evident atomic displacement, whereas the others remain relatively unchanged. One slip plane is formed between the topmost first and second atomic layers. The defect in Fig. 4(a) is assumed to be a cross-section of an edge dislocation with the dislocation line extending along the cutting edge.

On the Cu(110) and Cu(001) surfaces, at least two atomic layers are involved in the cutting process. With the advance of the cutting tool, the workpiece materials are randomly removed from the topmost atomic layers of workpiece surfaces. The removed workpiece atoms come

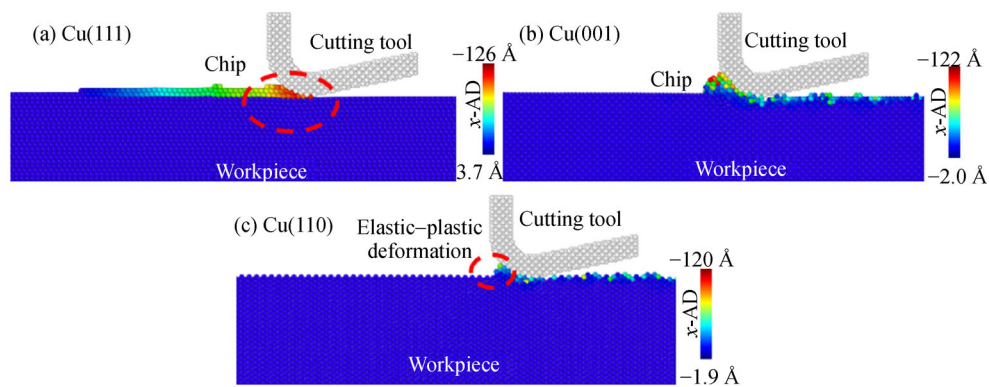


**Fig. 2** Chip formation on different crystallographic planes at the undeformed chip thickness of 0.2 nm and cutting edge radius of 2 nm. (a) Cu(111); (b) Cu(001); (c) Cu(110). The workpiece atoms are colored by their atomic displacements in the cutting direction ( $x$ -ADs).

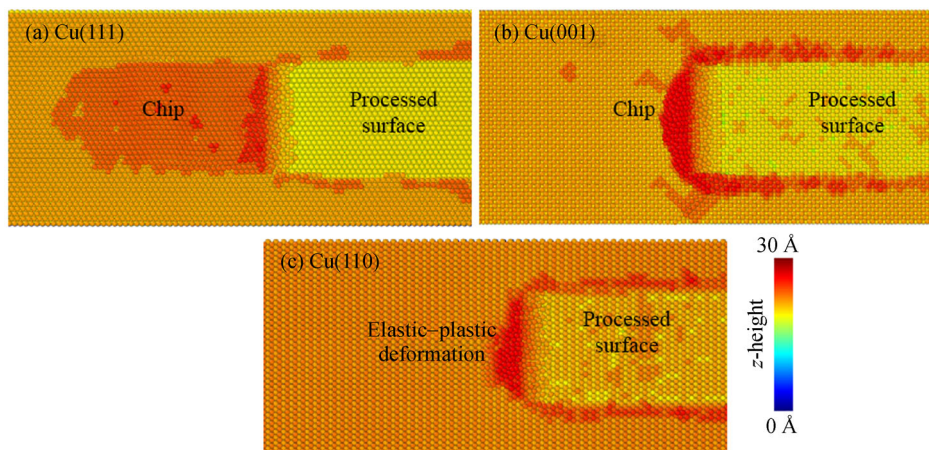


**Fig. 3** Simulation results on different crystallographic planes. (a) Cu(111); (b) Cu(001); (c) Cu(110). The cutting tool is omitted to clearly show the surface morphology of the processed surface.

from the targeted first atomic layer and other atomic layers. The newly formed processed surface consists of at least two atomic layers. These differences are due to the different atomic arrangement structures on each crystallographic planes, as further analyzed in Section 4.

### 3.3 Stress distribution analysis

A workpiece exhibits different stress distributions due to the crystallographic orientation effect. As shown in Fig. 5(a) and its closed-view, due to the translational motion of

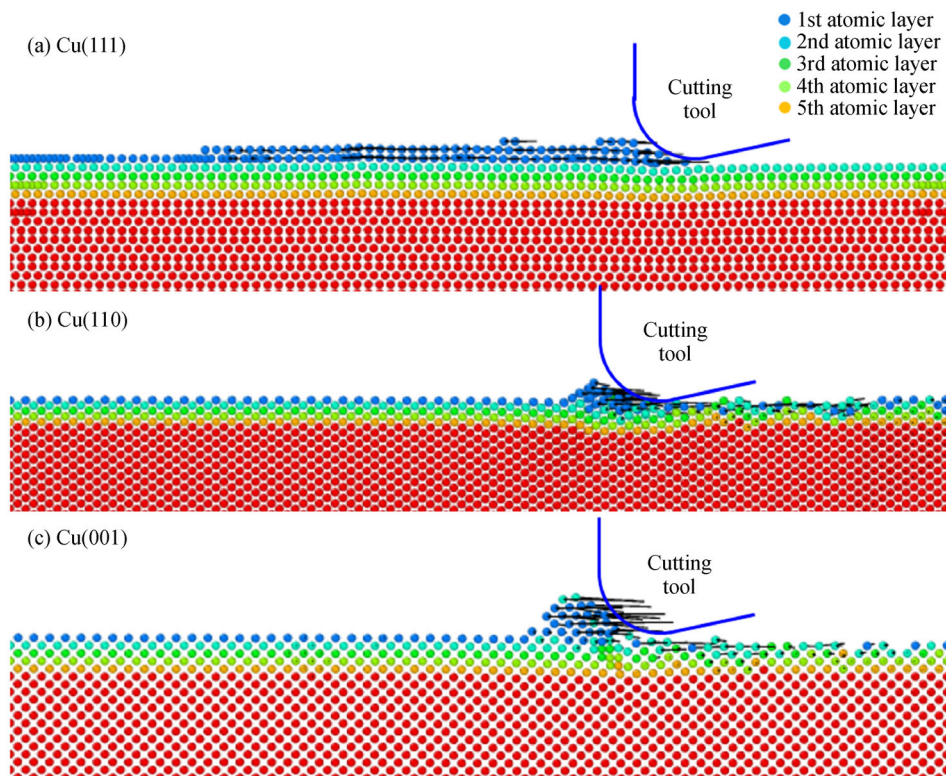


**Fig. 4** Atomic displacement vectors of workpiece materials on different crystallographic surfaces. (a) Cu(111); (b) Cu(110); (c) Cu(001).

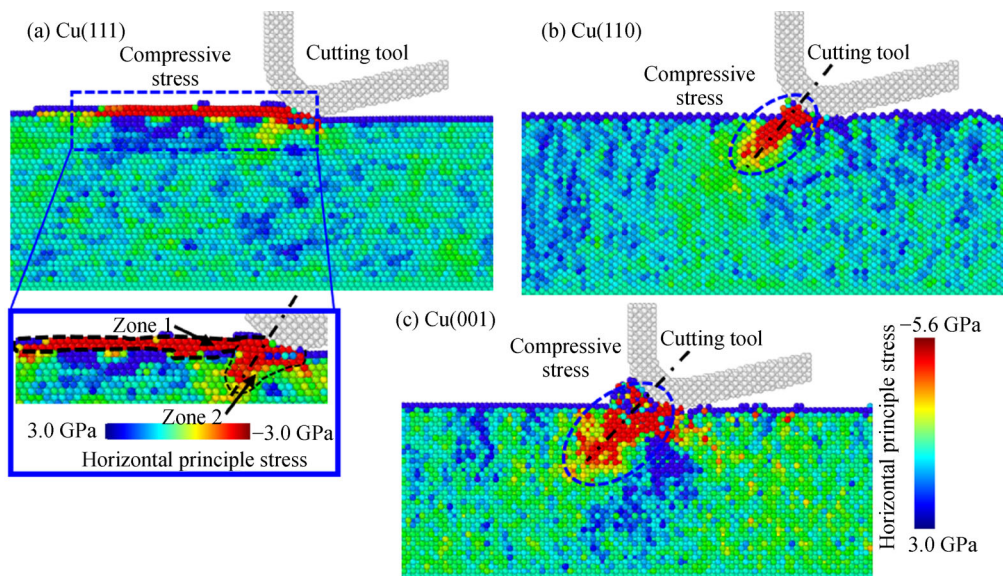


**Fig. 5** Crystallographic orientation effect on the first principle stress distribution. (a) Cu(111); (b) Cu(110); (c) Cu(001).

the cutting tool along the cutting direction, an evident concentration zone of horizontal principle stress is generated on the Cu(111) surface before the rounded cutting edge. This zone is further divided into Zones 1 and 2. Within Zone 1, the horizontal principle stress is imposed on the workpiece material ahead of the cutting edge radius, and it is highly localized across the undeformed cutting layer. The horizontal principle stress also deepens into the subsurface to form one concentration zone of compressive stress (Zone 2), which may induce workpiece subsurface deformation.

According to the MD trajectory files, Zone 1 has a higher compressive stress intensity than Zone 2. Thus, the horizontal principle stress is used to drive the plastic deformation in Zone 1 rather than in Zone 2. As analyzed in Section 3.2, material slip is conducted via dislocation within Zone 1. Therefore, on the Cu(111) surface, the horizontal compressive stress serves as the dominant driving force for chip formation by dislocation generation and motion.

By contrast, only one compressive stress concentration Zone 2 is formed on the Cu(001) and Cu(110) surfaces, but it has a larger area than the Zone 2 in the cutting on the Cu(111) surface. The crystallographic orientation effect changes the distribution state and further varies the material removal mechanisms. Different from the Cu(111) surface, the material removal on Cu(110) and Cu(001) surface is dominated by extrusion to form ruck accumulation (Figs. 4(b) and 4(c)).

As for vertical principle stress, Fig. 6 shows one compressive stress concentration zone on each analyzed case, despite different crystallographic orientations. This zone will provide the compressive stress to enable elastic

and/or plastic deformation along the vertical direction on the workpiece surface.

Figure 7 gives the workpiece shear stress distribution in the cutting process. One evident shear stress concentrated zone is generated on each surface, indicating that the shear action has an important effect on the workpiece subsurface and leads to subsurface deformation in the cutting. However, only several atomic layers and even a single atomic layer is involved in the cutting process. Thus, elastic deformation dominates the workpiece subsurface deformation process. By contrast, the Cu(110) and Cu(001) surfaces have a larger stress intensity than the Cu(111) surface. Therefore, achieving a defect-free processed surface by ACS cutting on the (110) and (111) planes of monocrystalline copper is difficult.

Overall, in the cutting-based single atomic layer removal process, the workpiece stress distribution has been evidently changed due to the crystallographic orientation effect. Consequently, two kinds of material removal mechanism exist in cutting-based single atomic layer removal process on the monocrystalline copper surface, i.e., the shear stress-driven dislocation motion mechanism on the Cu(111) surface and the extrusion mechanism on the Cu(001) and Cu(110) surfaces.

#### 3.4 Subsurface deformation mechanism

As analyzed in Section 3.3, in the cutting-based single atomic layer removal process, the workpiece stress state has been evidently changed due to the crystallographic orientation effect, thereby possibly inducing different subsurface deformations. In the ACS cutting on Cu(111) surface, no subsurface defect exists in the workpiece

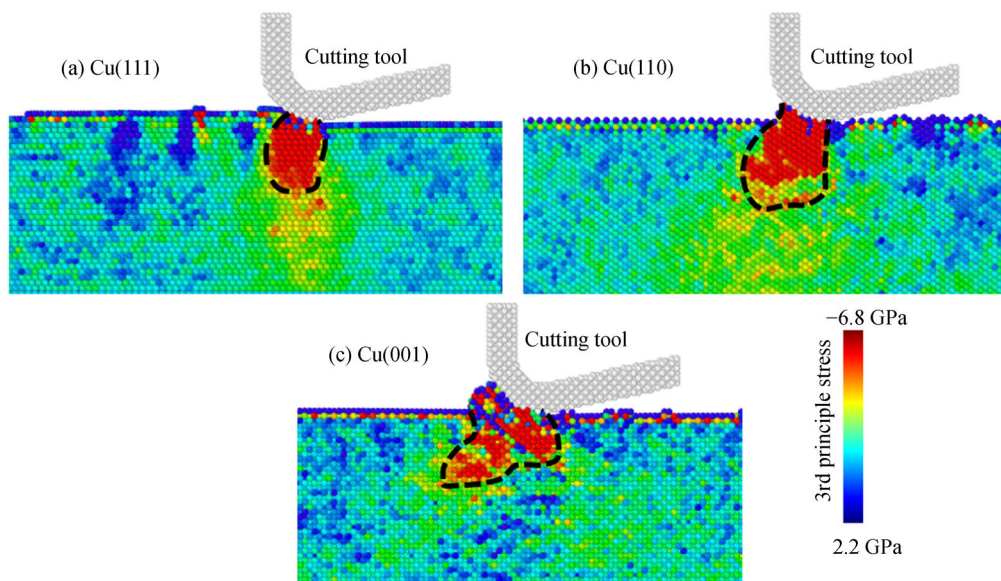
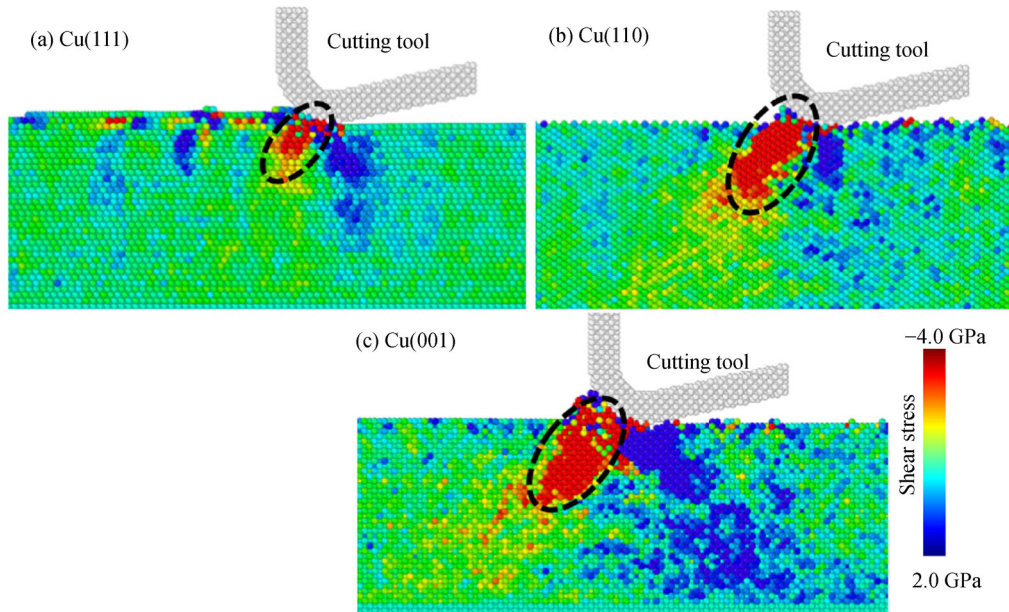


Fig. 6 Crystallographic orientation effect on vertical principle stress distribution. (a) Cu(111); (b) Cu(110); (c) Cu(001).



**Fig. 7** Crystallographic orientation effect on the shear stress distribution of workpiece. (a) Cu(111); (b) Cu(110); (c) Cu(001).

subsurface, and only elastic deformation is found on the processed surfaces [15]. After cutting, the elastically deformed part recovers completely and spontaneously. One issue arises due to the changed crystal orientation: How is the processed surface deformed in the cutting process on the different crystalline planes?

Figure 8 shows the workpiece subsurface defect structures in the cutting process. Some subsurface defects are generated in the workpiece subsurface and in the cutting on the Cu(110) and Cu(001) surfaces. These are due to the larger stress intensity generated in the cutting process, as analyzed in Section 3.3.

The generation of subsurface defects also means that elastic-plastic deformation would occur on the processed Cu(110) and Cu(001) surfaces. Therefore, due to the crystallographic orientation effect, different subsurface deformation mechanisms exist in the cutting process, i.e., elastic deformation and elastic-plastic deformation mechanisms.

## 4 Discussion

As analyzed above, when the materials to be cut are decreased to only a single atomic layer despite the same cutting conditions, including cutting edge radius, undeformed chip thickness, and cutting velocity, different cases of chip formation, surface generation, and workpiece stress distribution exist on various crystallographic planes. As illustrated in Fig. 9, two kinds of material removal mechanisms exist, namely, the dislocation motion-dominated material removal on close-packed crystal

plane and the extrusion-dominated material removal on other crystalline planes. Such difference is due to the crystallographic orientation effect on dislocation motion in the cutting process.

### 4.1 Crystallographic orientation effect on dislocation generation and motion

The material removal in ACS cutting is dominated by shear stress-driven dislocation motion. Thus, the cutting direction should be conducted along the crystallographic orientation, which facilitates the dislocation generation. Depending on the cutting direction and crystallographic orientation, three modes of dislocation generation and motion exist in the cutting process, further leading to different material removal mechanisms, as illustrated in Fig. 10.

On the Cu(111) surface in the ACS cutting, the dislocation is preferably generated parallel to the cutting direction, where the horizontal cutting force provides the shear stress to enable dislocation generation and motion, as shown in Fig. 10(a). Consequently, the material removal on this crystal plane is conducted in the form of chip formation by dislocation motion. By contrast, on the Cu(110) surface, the dislocation is preferably generated along the vertical direction, which is perpendicular to the cutting direction. As cutting distance increases, the materials are pressed downward under the action of the cutting tool to directly generate a new processed surface. Elastic-plastic deformation instead of chip formation exists within the contact region between the cutting tool and workpiece.

In the cutting on the Cu(001) surface, dislocations are

preferably generated along the direction that has an included angle with the cutting direction. Under the action of the cutting tool, the materials to be machined are partially removed in the form of chip formation via extrusion mechanisms, whereas others are formed into the new processed surfaces after elastic–plastic deformation.

Moreover, on the Cu(110) and Cu(001) surfaces, dislocation generation and motion easily exist in the workpiece subsurface, leading to subsurface defect generation in the cutting process. After cutting, the plastically deformed part finally leads to a lasting subsurface defect, as shown in Figs. 8(b) and 8(c).

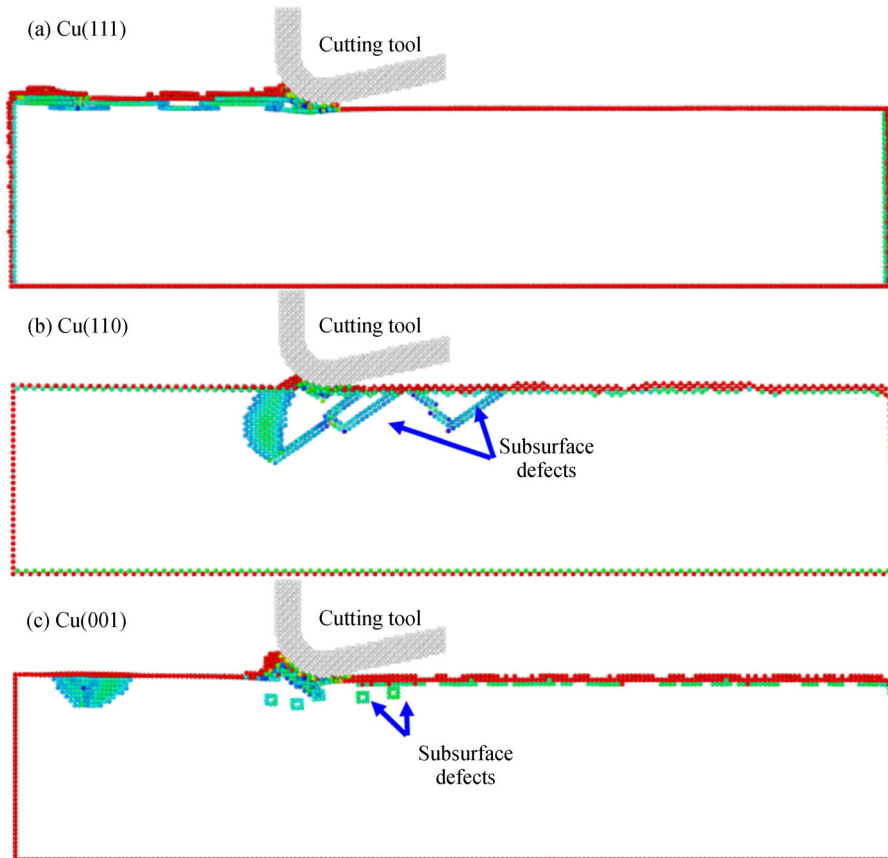


**Fig. 8** Subsurface defect structure on each processed surface. (a) Cu(111); (b) Cu(110); (c) Cu(001). The workpiece atoms are colored according to their centrosymmetry parameters (CSP). The atoms with a CSP of less than 3 are omitted to clearly visualize the subsurface defect.

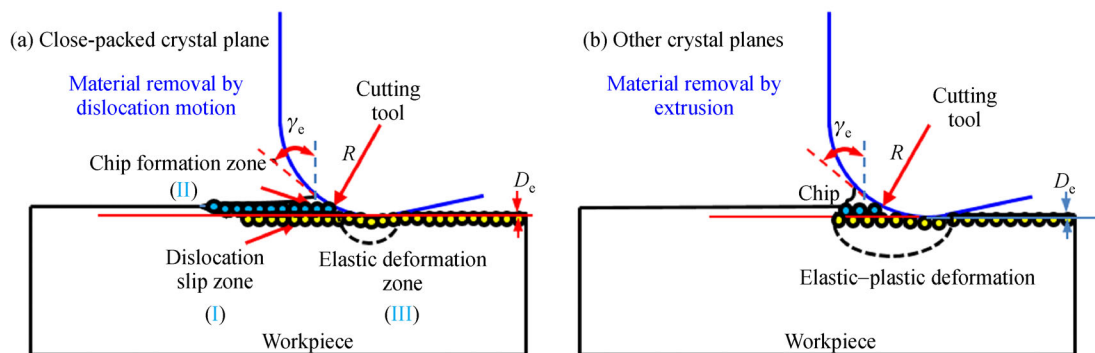


**Fig. 9** Schematic for the material removal mechanisms on different crystalline planes. (a) Close-packed crystal plane; (b) other crystal planes.

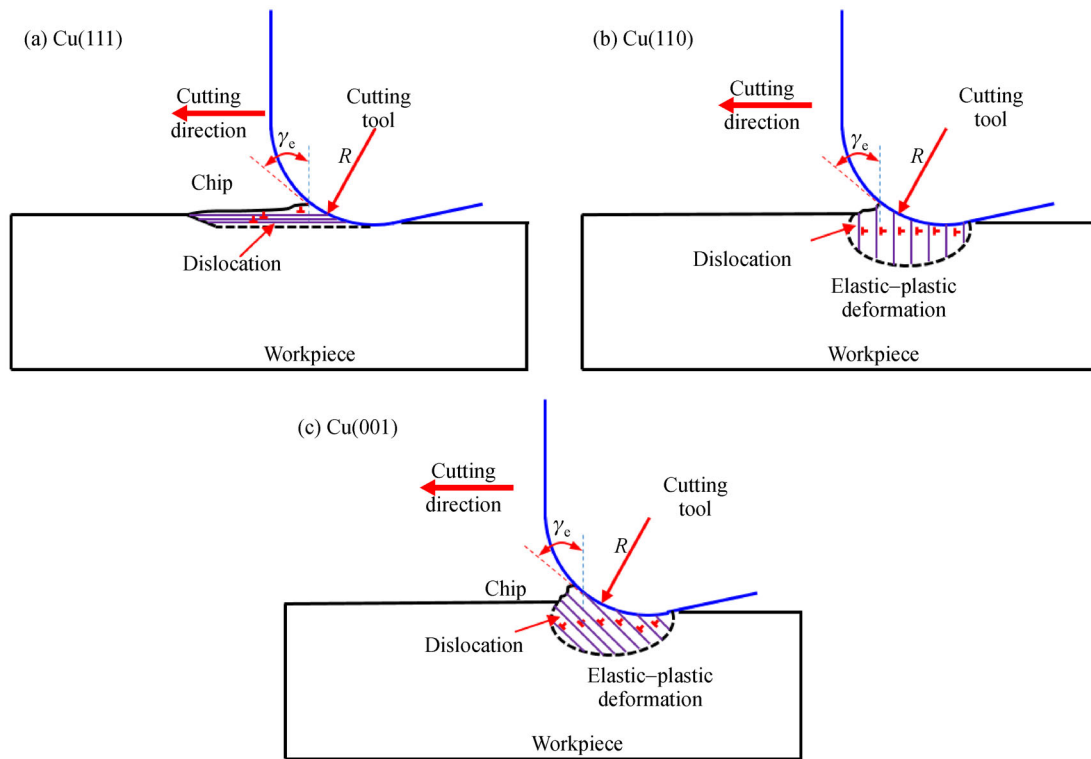


**Fig. 10** Schematic for three types of dislocation generation and motion in ACS cutting. (a) Cu(111); (b) Cu(110); (c) Cu(001).

#### 4.2 Atom arrangement structure on dislocation generation

The occurrence of different modes of dislocation generation and motion is ascribed to different atomic arrangement structure on each crystallographic plane. For face centered cubic (FCC) metal materials (Fig. 11), different interlayer spacing distances ( $d$ ) exist on various crystalline planes.

On the close-packed crystal plane, like the (111) plane, one very-small overlapped zone exists between the topmost neighboring atomic layers due to the larger interlayer spacing distance. When the cutting tool comes in contact with the atomic layers included in undeformed chip thickness, those atomic layers would easily slip along the cutting direction. By contrast, on the non-close packed crystalline plane, such as (001) or (110) plane, the distance of the overlapped zone is evidently increased because of the lower  $d_{\text{layer}}$ . Consequently, the interplay actions between neighboring atomic layers tend to grow, against realizing the controlled removal of the targeted atomic layer. Moreover, different interatomic distances ( $b$ ) exist within each atomic layer on different crystal planes, which affect the material deformation and removal process. As illustrated in Fig. 11(a), on the (111) plane, the atoms within each atomic layer are closely linked, and the interatomic distance in-layer ( $b$ ) equals  $2r_w$ . Any atomic motion of one atom has an important influence on its neighboring atoms in the first atomic layer. By contrast, on

the (001) plane, the interatomic distance in-layer is larger than  $2r_w$ , and the atoms within one atomic layer are not closely adjacent. Any atomic motion of one atom in the first atomic layer would first directly induce the motion of atoms in the second layer. At least two atomic layers are involved in the cutting-based single atomic layer removal process. Furthermore, on the (111) plane, the atoms in the first atomic layer directly come in contact with those in the second and third atomic layers at the same time. In cutting, at least three atomic layers are expected to be involved.

In the cutting process, the atoms within the first atomic layer are under different force conditions due to different atomic arrangement structures. As illustrated in Fig. 12, on the (111) surface, under the action of rounded cutting edge, the targeted atom is subjected to a cutting force imposed by cutting tool ( $F_R$ ), a drag force from the atoms within the second atomic layer ( $F_D$ ), and a horizontal cutting force from other atoms within the first atomic layer ( $F_H$ ). Therefore, in the cutting process, the atomic displacement behavior of the targeted atom on the close-packed crystal plane is the result of  $F_R$ ,  $F_D$ , and  $F_H$ .

Different from the Cu(111) surface, the atoms within the targeted first atomic layer on the Cu(001) surface are only subjected to  $F_R$  and  $F_D$  in the 2D orthogonal cutting process. To achieve the removal of the targeted atom, the fact that both materials yield strength in the cutting and normal directions should be overcome. On the Cu(110)

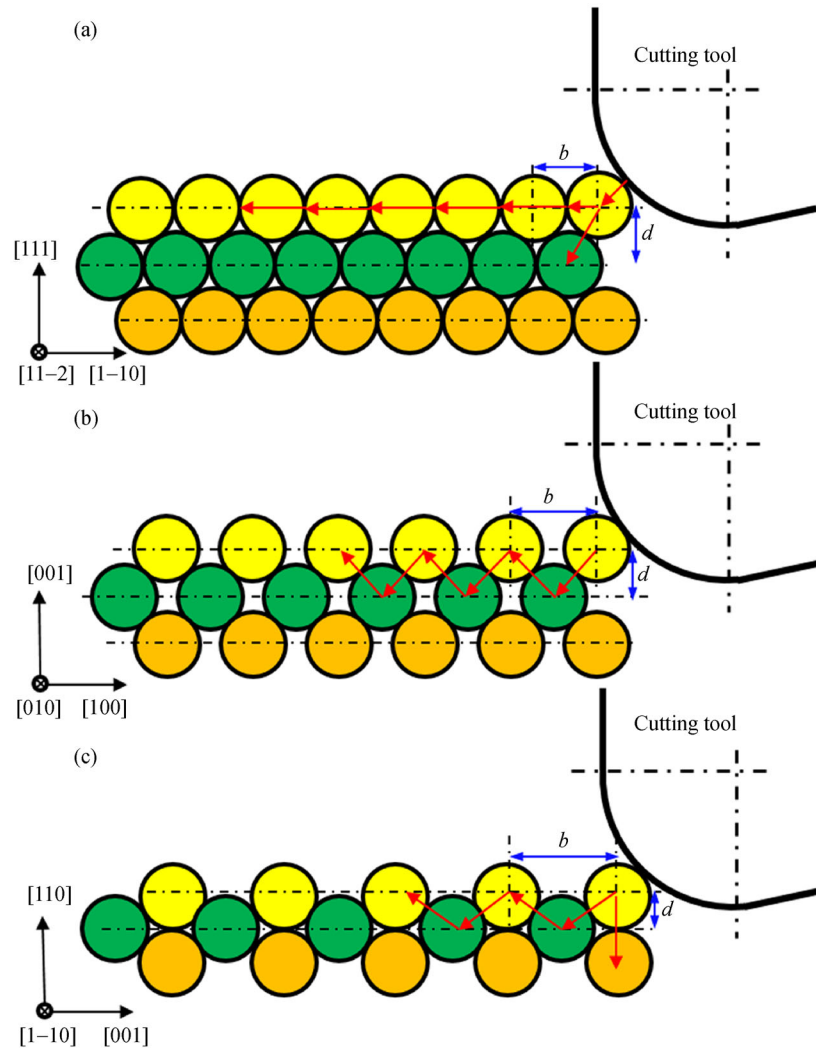


**Fig. 11** Atomic arrangement structures of (111), (001), and (110) surfaces of the FCC metal materials. (a) Cu(111); (b) Cu(001); (c) Cu(110).

surface, aside from  $F_R$  and  $F_D$ , a force from the third atomic layer is also imposed on the first atomic layer.

On the close-packed crystalline plane, when the shear stress imposed on the first atomic layer is larger than the critical resolved shear stress (CRSS), the targeted first atomic layer tends to slip over the second atomic layer, thereby generating dislocation. In the cutting process, the cutting force provides shear stress to enable dislocation generation. As shown in Fig. 5(a), in the cutting process on Cu(111) surface, the horizontal principle stress serves as the shear stress, which enables material slip along the cutting direction. As further determined by the plot of cutting forces versus cutting distance in Fig. 13, with the advance of the cutting tool, material deformation and removal easily occur via dislocation motion when the cutting-induced horizontal principle stress is larger than the CRSS of the workpiece material.

As shown in Fig. 13(a), on Cu(111) surface, the tangential component of cutting force is much smaller

than the normal cutting force, indicating that a lower tangential cutting force could enable material removal by chip formation via dislocation motion, especially material slip (Fig. 4(a)). On the (001) and (110) surfaces, the atoms within the first atomic layer are not closely adjacent. In the cutting process, the cutting edge intermittently comes in contact with the atoms within the first atomic layer. Thus, the cutting forces exhibit a larger fluctuation than those on the Cu(111) surface, as shown in Figs. 13(b) and 13(c). Moreover, on the Cu(110) surface, under the action of the cutting tool, the materials within the first atomic layer can be easily pressed into the processed surface, as the [110] direction is its close-packed crystallographic orientation.

From the above analysis, the material deformation and removal process in ACS cutting at the atomic scale could be regarded as the cutting tool-based displacement behavior of the specific atomic layer. The key to enabling controlled cutting-based material removal at the atomic scale is to accurately control the motion of the targeted

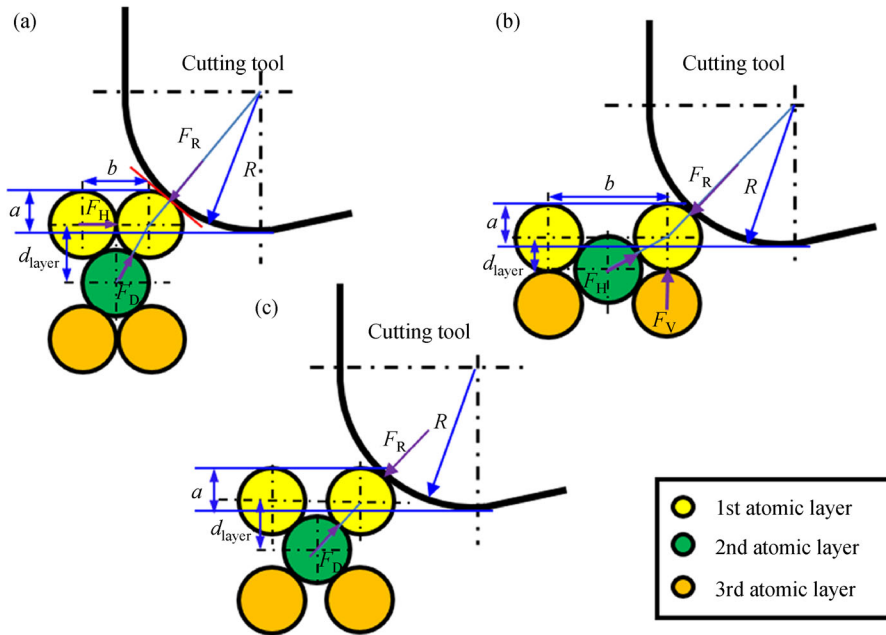


**Fig. 12** Force condition of the targeted atom in round-edged tool-based cutting. (a) Cu(111); (b) Cu(110); (c) Cu(001).

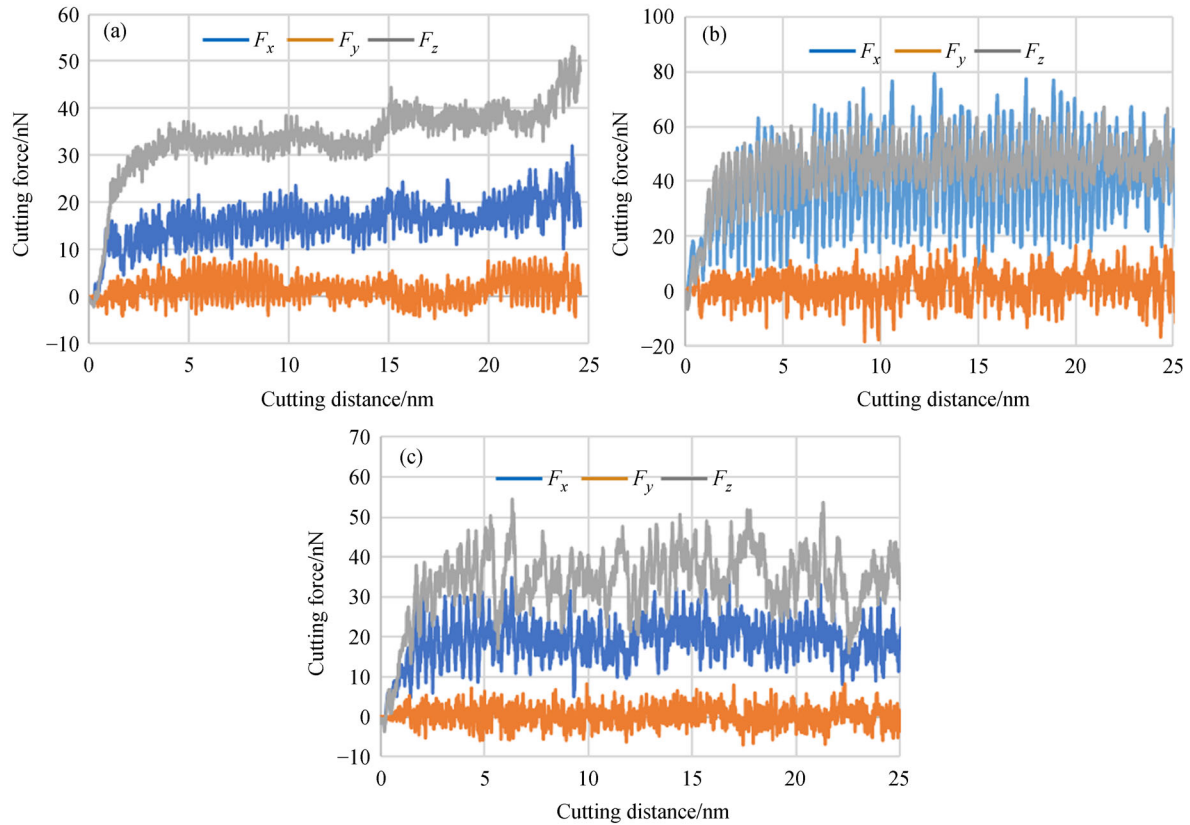


**Fig. 13** Plots of cutting force versus cutting distance on each analyzed crystal planes. (a) Cu(111); (b) Cu(001); (c) Cu(110).

atoms or atomic layer with the aid of the cutting tool. For this reason, the interatomic effect of atoms within one atomic layer and the interlayer effect of neighboring atomic layers need to be considered when the materials to be machined only include several atomic layers and even one atomic layer.

Overall, the crystallographic orientation effect on ACS cutting needs to be ascribed to the different atomic arrangement structure on each crystal planes. It affects the forced condition of each atom in the cutting process by inducing different atomic motion of each atomic layer and by changing the dislocation generation and evolution. Consequently, on different crystallographic planes, two kinds of material removal mechanisms exist in atomic-scale cutting.

## 5 Conclusions

The crystallographic orientation effect on cutting-based single atomic layer removal mechanism of monocrystalline copper is investigated through MD analysis. The research findings indicate that due to the crystallographic orientation effect, two kinds of material removal mechanisms exist in the single atomic layer cutting, namely, dislocation motion and extrusion. Defect-free processed surfaces can be obtained through cutting-based material removal by shear stress driven-dislocation motion rather than by extrusion. The main conclusions are summarized as follows:

1) When the undeformed chip thickness is decreased to the atomic scale, two kinds of cutting-based material removal mechanisms arise on different crystallographic surfaces, namely, extrusion and shear stress-driven dislocation motion mechanisms. Material removal needs to be conducted in the form of dislocation motion mechanism rather than extrusion mechanism to obtain an atomic and defect-free processed surface.

2) The workpiece stress distribution is evidently changed by the crystallographic orientation effect. On the Cu(001) surface, the horizontal principle stress serves as a shear stress, which enables material slip by dislocation motion. On the Cu(110) and Cu(111) surfaces, under the action of the cutting tool, one compressive stress concentration zone is formed to realize material removal dominated by extrusion.

3) On the close-packed crystalline plane, material removal is dominated by shear stress-driven dislocation motion. On other non-close-packed crystalline planes, when the materials to be machined are composed of only a single atomic layer, the extrusion action dominates the final material removal.

4) Crystallographic orientation effect induces different subsurface deformation mechanisms in the cutting-based single atomic layer removal process. Elastic-plastic deformation occurs on the processed Cu(110) and

Cu(001) surfaces, which differs from the elastic deformation on the processed Cu(111) surface.

5) The crystallographic orientation effect on the material removal behavior in ACS cutting is ascribed to different atomic arrangement structures. A larger interlayer spacing distance exists between neighboring atomic layers on close-packed crystal planes than on non-close packed crystalline planes, facilitating the controlled removal of the first atomic layer.

6) Atomic- and close-to-atomic-scale cutting should be conducted on the close-packed crystallographic planes of FCC metal materials to obtain the defect-free processed surfaces.

**Acknowledgements** The authors would like to thank the financial support from the Science Foundation Ireland (Grant No. 15/RP/B3208) and the '111' Project by the State Administration of Foreign Experts Affairs and the Ministry of Education of China (Grant No. B07014).

## References

1. Fang F Z. Atomic and close-to-atomic scale manufacturing: Perspectives and Measures. *International Journal of Extreme Manufacturing*, 2020, 2: 030201
2. Fang F Z, Zhang N, Guo D, et al. Towards atomic and close-to-atomic scale manufacturing. *International Journal of Extreme Manufacturing*, 2019, 1(1): 012001
3. Yan J, Asami T, Harada H, et al. Crystallographic effect on subsurface damage formation in silicon microcutting. *CIRP Annals*, 2012, 61(1): 131–134
4. Chae J, Park S S, Freiheit T. Investigation of micro-cutting operations. *International Journal of Machine Tools and Manufacture*, 2006, 46(3–4): 313–332
5. Egashira K, Furukawa T, Yamaguchi K, et al. Microcutting using a micro turn-milling machine. *Precision Engineering*, 2016, 44: 81–86
6. O'Connor B P, Marsh E R, Couey J A. On the effect of crystallographic orientation on ductile material removal in silicon. *Precision Engineering*, 2005, 29(1): 124–132
7. Xue B, Geng Y Q, Wang D, et al. Improvement in surface quality of microchannel structures fabricated by revolving tipbased machining. *Nanomanufacturing and Metrology*, 2019, 2(1): 26–35
8. Fang F Z, Wu H, Zhou W, et al. A study on mechanism of nano-cutting single crystal silicon. *Journal of Materials Processing Technology*, 2007, 184(1–3): 407–410
9. Fang F Z, Xu F, Lai M. Size effect in material removal by cutting at nano scale. *International Journal of Advanced Manufacturing Technology*, 2015, 80(1–4): 591–598
10. Fang F Z, Wu H, Liu Y. Modelling and experimental investigation on nanometric cutting of monocrystalline silicon. *International Journal of Machine Tools and Manufacture*, 2005, 45(15): 1681–1686
11. Masuzawa T. State of the art of micromachining. *CIRP Annals*, 2000, 49(2): 473–488
12. Fang F Z, Zhang X, Gao W, et al. Nanomanufacturing—Perspective

- and applications. *CIRP Annals*, 2017, 66(2): 683–705
13. Joshi S S. Ultraprecision machining (UPM). In: Bhushan B, ed. *Encyclopedia of Nanotechnology*. Dordrecht: Springer, 2016
  14. Xie W K, Fang F Z. Cutting-based single atomic layer removal mechanism: Atomic sizing effect. *Nanomanufacturing and Metrology*, 2019, (2): 241–252
  15. Xie W K, Fang F Z. Mechanism of atomic and close-to-atomic scale cutting of monocrystalline copper. *Applied Surface Science*, 2020, 503: 144239
  16. Xie W K, Fang F Z. Effect of tool edge radius on material removal mechanism in atomic and close-to-atomic scale cutting. *Applied Surface Science*, 2020, 504: 144451
  17. Xie W K, Fang F Z. Cutting-based single atomic layer removal mechanism of monocrystalline copper: Edge radius effect. *Nanoscale Research Letters*, 2019, 14(1): 370
  18. Mathew P T, Rodriguez B J, Fang F Z. Atomic and close-to-atomic scale manufacturing: A review on atomic layer removal methods using atomic force microscopy. *Nanomanufacturing and Metrology*, 2020, 3: 167–186
  19. Goel S, Kovalchenko A, Stukowski A, et al. Influence of microstructure on the cutting behaviour of silicon. *Acta Materialia*, 2016, 105: 464–478
  20. Chavoshi S Z, Goel S, Luo X. Molecular dynamics simulation investigation on the plastic flow behaviour of silicon during nanometric cutting. *Modelling and Simulation in Materials Science and Engineering*, 2015, 24(1): 015002
  21. Shimada S, Ikawa N, Tanaka H, et al. Feasibility study on ultimate accuracy in microcutting using molecular dynamics simulation. *CIRP Annals*, 1993, 42(1): 91–94
  22. Goel S, Stukowski A, Luo X, et al. Anisotropy of single-crystal 3C–SiC during nanometric cutting. *Modelling and Simulation in Materials Science and Engineering*, 2013, 21(6): 065004
  23. Lai M, Zhang X, Fang F Z. Crystal orientation effect on the subsurface deformation of monocrystalline germanium in nanometric cutting. *Nanoscale Research Letters*, 2017, 12(1): 296
  24. Chen L, Wen J, Zhang P, et al. Nanomanufacturing of silicon surface with a single atomic layer precision via mechanochemical reactions. *Nature Communications*, 2018, 9(1): 1542
  25. Zhu P, Fang F Z. Study of the minimum depth of material removal in nanoscale mechanical machining of single crystalline copper. *Computational Materials Science*, 2016, 118: 192–202
  26. Yuan Z J, Lee W B, Yao Y X, et al. Effect of crystallographic orientation on cutting forces and surface quality in diamond cutting of single crystal. *CIRP Annals*, 1994, 43(1): 39–42
  27. Lawson B L, Kota N, Ozdoganlar O B. Effects of crystallographic anisotropy on orthogonal micromachining of single crystal aluminum. *Journal of Manufacturing Science and Engineering*, 2008, 130(3): 031116
  28. Lee W B, To S, Sze Y K, et al. Effect of material anisotropy on shear angle prediction in metal cutting—A mesoplasticity approach. *International Journal of Mechanical Sciences*, 2003, 45(10): 1739–1749
  29. Fang F Z, Xu F. Recent advances in micro/nano-cutting: Effect of tool edge and material properties. *Nanomanufacturing and Metrology*, 2018, 1(1): 4–31
  30. Komanduri R, Chandrasekaran N, Raff L M. MD simulation of nanometric cutting of single crystal aluminum—Effect of crystal orientation and direction of cutting. *Wear*, 2000, 242(1–2): 60–88
  31. Komanduri R, Chandrasekaran N, Raff L M. Orientation effects in nanometric cutting of single crystal materials: An MD simulation approach. *CIRP Annals-Manufacturing Technology*, 1999, 48(1): 67–72
  32. Wu X, Li L, He N, et al. Investigation on the influence of material microstructure on cutting force and bur formation in the micro cutting of copper. *International Journal of Advanced Manufacturing Technology*, 2015, 79(1–4): 321–327
  33. Xu F, Fang F Z, Zhu Y, et al. Study on crystallographic orientation effect on surface generation of aluminum in nano-cutting. *Nanoscale Research Letters*, 2017, 12(1): 289
  34. Plimpton S. Fast parallel algorithms for short-range molecular dynamics. *Journal of Computational Physics*, 1995, 117(1): 1–19
  35. Foiles S M, Baskes M I, Daw M S. Embedded-atom-method functions for the fcc metals Cu, Ag, Au, Ni, Pd, Pt, and their alloys. *Physical Review B*, 1986, 33(12): 7983–7991
  36. Zhang L, Tanaka H. Towards a deeper understanding of wear and friction on the atomic scale—A molecular dynamics analysis. *Wear*, 1997, 211(1): 44–53